Investigation of the Structural Stability of Cardiotoxin Analogue III from the Taiwan Cobra by Hydrogen−Deuterium Exchange Kinetics†

Thirunavukkarasu Sivaraman, Thallampuranam Krishnaswamy S. Kumar, and Chin Yu*

Department of Chemistry, National Tsing Hua University, Hsinchu, Taiwan

Received January 20, 1999; Revised Manuscript Received May 21, 1999

ABSTRACT: The conformational stability of a small (∼7 kDa), all β-sheet protein, cardiotoxin analogue III (CTX III), from the venom of the Taiwan cobra has been investigated by hydrogen−deuterium (H/D) exchange using two-dimensional NMR spectroscopy. The H/D exchange kinetics of backbone amide protons in CTX III has been monitored at pD 3.6 and 6.6 (at 25 °C), for over 5000 h. Examination of H/D exchange kinetics in the protein showed that a number of slowly exchanging residues are in the hydrophobic core of the protein. The average protection factor of the amide protons of residues belonging to the triple-stranded β-sheet domain is about 20 times greater than that of those in the double-stranded β-sheet segment. The residues in the C-terminal tail of the molecule, though structureless, have been found to exhibit significant protection against H/D exchange. Comparison of the quenched-flow H/D exchange data on CTX III with those obtained in the present study reveals that the most slowly exchanging portion constitutes the folding core of the protein.

The fundamental forces governing the conformational stability of proteins in solution are still not completely understood. Although valuable information could be obtained from conventional methods such as denaturant titration and calorimetric measurements, very little information is available on the conformational dynamics of proteins in solution. In this context, hydrogen−deuterium (H/D)[1] exchange has become an important tool in the study of structure, stability, folding dynamics and intermolecular interactions in protein systems in solution (*1*−*4*). H/D exchange data for proteins directly indicate the relative accessibility of various protons to solvent (*5*, *6*). H/D experiments derive advantage of the fact that the hydrogen bonded amide protons exchange with solvent at several orders of magnitude slower than which are non-hydrogen bonded (*7*, *8*). Large differences in the rates of exchange of hydrogen-bonded residues could be observed (*9*−*12*). The significant differences are a direct measurement of the local stability, which permits an assessment of the local rigidity or the flexibility in the protein molecule. The detailed structural stability information of a protein at the residue level could be obtained by measuring the hydrogen exchange kinetics of individual residues (*13*, *14*).

The H/D exchange of proteins in their folded state is generally believed to follow the two-step model (*15*, *16*). According to this model, a protein is believed to be in two sets of conformations, closed and open, in equilibrium with each other. However, solvent exchange only takes place from the open state:

$$\text{closed} \underset{k_{op}}{\overset{k_{cl}}{\rightleftharpoons}} \text{open} \xrightarrow{k_{int}} \text{exchange}$$

where k_{op} and k_{cl} are the rate constants for the opening and closing conformations and k_{int} is the exchange rate in the random coil conformational state. The observed exchange rate, k_{ex}, is given by $k_{op}k_{int}/(k_{cl} + k_{int})$.

There are two kinetic limits for exchange (*17*−*19*). The first limit (EX1) occurs when $k_{cl} \ll k_{int}$. The resulting observed exchange rate, k_{ex}, is equivalent to k_{op}. The second limit (EX2) occurs if conformational closing is faster than solvent exchange from open state ($k_{cl} \gg k_{int}$). The intrinsic exchange in open state $k_{ex} = (k_{op}/k_{cl})k_{int} = K_{eq}k_{int}$ (where K_{eq} is defined as the equilibrium constant for the conformational transition between open and closed states). Thus, under EX2 conditions, the exchange kinetics can be used to study the equilibrium between the open and closed states. Since the intrinsic rate (k_{int}) of exchange from the open state can be predicted from the unstructured peptide data, the standard free energy change of the opening reaction can be reliably estimated as $\Delta G_{ex} = -RT \ln K_{eq}$ (where $K_{eq} = k_{ex}/k_{int}$), where ΔG_{ex} is the free energy for the opening process, R is the gas constant, and T is the temperature in kelvins.

The two extreme cases of the two-step exchange model are limited local fluctuations and complete global unfolding (*20*−*22*). The slowest exchanging amide protons are generally believed to exchange by the global unfolding pathway. In addition, for these residues, the free energy of exchange (ΔG_{ex}) estimated from the H/D experiments is expected to be similar to the free energy change calculated from the equilibrium unfolding experiments (*23*, *24*) monitored by optical methods. On the other hand, the faster exchanging

† This work was supported by the National Science Council, Taiwan (NSC 88-2311-B-007-021 and NSC 88-2113-M-007-028) and Dr. C. S. Tsong Memorial Medical Research Foundation (VGHTH-87-09-2).

* To whom correspondence should be addressed: Fax +886 35 711082; E-mail cyu@chem.nthu.edu.tw.

[1] Abbreviations: CTX III, cardiotoxin III.; CheY protein, chemotactic protein; CD, circular dichroism; CI2, chymotrypsin inhibitor; GdnHCl, guanidine hydrochloride; H/D, hydrogen/deuterium; NMR, nuclear magnetic resonance; RNase, ribonuclease.

10.1021/bi9901230 CCC: $18.00
Published on Web 07/16/1999

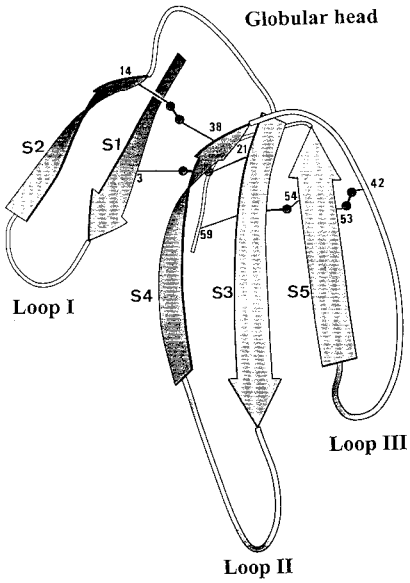

FIGURE 1: MOLSCRIPT representation of the solution structure of CTX III depicting the overall backbone-folding. The ribbon arrows represent regions of the peptide backbone in the β-sheet conformation. S1−S5 represent the various β-strands in the structure of CTX III. The disulfide bonds in the protein are located between residues 3 and 21, 14 and 38, 42 and 53, and 54 and 59.

amides are assumed to exchange through the local fluctuations. The ΔG_{ex} values for these residues are predicted to be lower than the average free energy of unfolding (ΔG_u), because the exchange that would occur from an intermediate need not be necessarily dependent on global stability.

Cardiotoxin analogue III (CTX III) is a small molecular weight (~7 kDa), highly basic, all β-sheet protein, cross-linked by four disulfide bridges (Figure 1, *25*−*30*). The secondary structural elements in the protein include antiparallel double- and triple-stranded β-sheet domains (*27*). Refolding kinetics of this protein has been recently investigated by the quenched-flow hydrogen−deuterium technique (*32*). In the present study, we critically evaluate the conformational stability of CTX III by the H/D exchange technique. In addition, we also examine the relationship between the chronology of events in the kinetic folding pathway and the native-state hydrogen exchange kinetics of CTX III.

MATERIALS AND METHODS

CTX III was purified from the crude Taiwan cobra venom (*Naja naja atra*) by the procedure described by Yang et al. (*33*). D_2O was purchased from Cambridge Isotope Laboratories. Ultrapure guanidine hydrochloride (GdnHCl) was purchased from Sigma Chemical Co. All other chemicals used in this study were of high-quality analytical grade.

Circular Dichroism. The guanidine hydrochloride-induced equilibrium unfolding of CTX III was followed by far- and near-ultraviolet circular dichroism (CD) spectroscopy. CD measurements were carried out with 0.2 and 1 mm path length quartz cells. The GdnHCl denaturation of CTX III (160 μM) was monitored in a deuterated solution, at pD 3.6. Each spectrum was an average of at least five scans. Necessary background corrections were made in all the spectra. CD spectra were recorded on a Jasco J720 spectropolarimeter and the sample temperature was maintained with a Neslab RTE-110 circulating water bath at 25 ± 0.2 °C. The data analysis was performed by well-established procedures (*34*).

NMR Spectra and Amide Proton Exchange. All ^{1}H NMR spectra were recorded on a Bruker DMX-600 spectrometer. The temperature of the spectrometer was calibrated with 100% or 4% methanol in methanol-d_4. For each sample, the temperature was calibrated prior to data acquisition.

The exchange kinetics of the amide protons in the protein (CTX III) was monitored by recording magnitude COSY spectra of the sample. The sample for amide proton exchange kinetics measurements was prepared by dissolving the lyophilized CTX III in deuterated buffer at pD 3.6 and 6.6 (at 25 °C). The concentration of the protein samples were ~2 mM. Typical data acquisition parameters were 16 transients of 1024 data points and 256 t_1 increments with water suppression by presaturation. Prior to Fourier transformation, the data were multiplied by a sine-squared function in the t_1 and t_2 dimension. The spectral assignments were based on the chemical shift data reported by Bhaskaran et al. (*27*) and Sivaraman et al. (*28*). Cross-peak intensities were measured by volume integration. Each spectrum was internally referenced to nonexchangeable aromatic cross-peaks ($C^{\delta}H-C^{\epsilon}H$ of Tyr51 and Phe25). Peak volumes were fit to a single-exponential function, $Y = A_0 \exp^{-kt} + C$, where C is the baseline noise and which takes into account the residual nondeuterated water and the threshold setting used in the intensity calculations. For some residues, the amide proton decay was fitted to the single-exponential function without inclusion of the baseline noise correction factor C. The curve fitting was done with the KaleidaGraph software (Synergy Software) on a personal IBM computer. The intrinsic rate constants of exchange (k_{int}) for each amide proton at different values of pH were calculated according to the reported equation from model peptides, taking into account the activation enthalpies (*35*).

The protection factor (P) for the various amide protons in the protein were estimated on the basis of the method reported by Bai et al. (*35*), using

$$P = k_{int}/k_{ex}$$

where k_{int} and k_{ex} represent the exchange rates of the protein in the random coil and native conformational states, respectively. The free energy of exchange of the amide protons was calculated from the equation $\Delta G_{ex} = -RT \ln (k_{ex}/k_{int})$, where R is the gas constant and T is the absolute temperature at which the exchange was monitored.

RESULTS

Proteins generally exhibit higher stability in D_2O. For this reason, the equilibrium denaturation experiments were performed in D_2O. The guanidine hydrochloride-induced unfolding of CTX III was monitored by far-ultraviolet (190−250 nm) circular dichroism spectroscopy. The native spectrum shows a negative ellipticity CD band centered at around 213 nm, indicative of the backbone of the protein being in the β-sheet conformation. Figure 2 depicts the percentage of unfolded species based on changes in the ellipticity at 213 nm of the protein (CTX III) with increasing concentrations of GdnHCl. It could be observed that no significant change occurs up to 3.5 M GdnHCl concentration. However, beyond 3.5 M GdnHCl, the protein begins to unfold (Figure

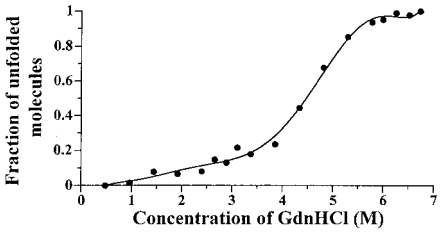

FIGURE 2: Fraction of unfolded species in CTX III detected by CD. The fraction of unfolded species was estimated on the basis of the ellipticity changes at 213 nm.

2). The unfolding of the protein is complete at a GdnHCl concentration of 5.8 M. The unfolding profile monitored through the ellipticity changes at 270 nm (which is representative of the tertiary structural contacts in the protein) is almost superimposable with that obtained from the 213 nm ellipticity changes (data not shown). This aspect implies that the unfolding of the protein under these conditions follows a two-state transition. The free energy change of unfolding the protein (ΔG_u) is found to be 6.0 kcal·mol^{-1}. The *m* value, which is a measure of the cooperativity of unfolding, is estimated to be 0.74 kcal·mol^{-1}·M^{-1}. In addition, the concentration (C_m) at which half of the protein molecules are unfolded is calculated to be 4.7 M.

CTX III is a 60 amino acid protein, with five proline residues (*25*). Hence, in theory, there are 55 backbone amide protons whose H/D exchange kinetics could be monitored. The H/D exchange of CTX III was monitored at 25 °C in 500 mM glycine deuterochloride buffer (pD = 3.6). The H/D exchange was monitored by using a series of magnitude COSY spectra in the time range from 15 min to >5000 h. The assignments of the various cross-peaks in the fingerprint region (NH−C$^{\alpha}$H) were the same as reported earlier (*27*, *28*). Minor shift(s) due to the difference(s) in temperature and pH were verified by standard sequential assignment procedures.

Of the 55 amide protons, 11 exchanged within the dead time of the experiment (20 min). These 11 residues are located in the surface-exposed, unstructured portion of the molecule. Magnitude COSY spectra of the protein recorded after 20 h of exchange reveals that only 29 residues are protected from exchange. The residues that exchange out within the first 20 h of exchange include Leu6, Leu9, Thr13, Cys14, Asn19, Ala28, Thr29, Lys31, Lys44, Ser46, and Val49. Interestingly, some of the residues involved in the β-sheet conformation also exchanged significantly within this time span. These include Phe10 and Lys12, which belong to the double-stranded β-sheet segment. In addition, Arg36 and Cys53, which are a part of the triple-stranded β-sheet domain, are found to substantially exchange within 20 h. With the exception of Val27, Val34, and residues located at the C-terminal end (residues 57−59), most of the residues not involved in secondary structure formation are exchanged out within the first 100 h of exchange (Figure 3). A majority of the residues involved in the β-sheet conformation are prominently exchanged only at time periods greater than 300 h (Figure 4). The magnitude COSY spectra of the protein dissolved in D_2O and recorded after 1000 h shows only eight cross-peaks. These correspond to the amide protons of Cys21, Tyr22, Lys23, Met24, Lys35, Ile39, Val52, and Cys54. Coincidentally, all these residues belong to the triple-stranded β-sheet domain.

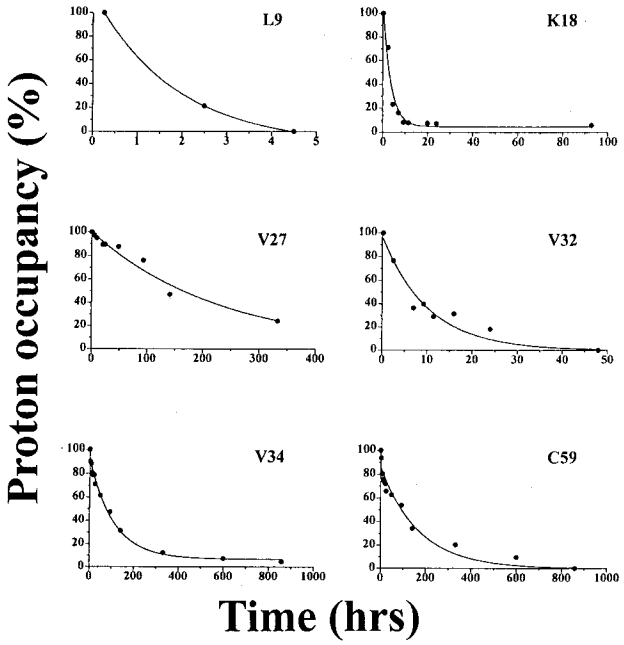

FIGURE 3: Time course of amide proton exchange (percentage of proton occupancy) of some residues in the unstructured portions of the CTX III molecule. The exchange was monitored at pD 3.6.

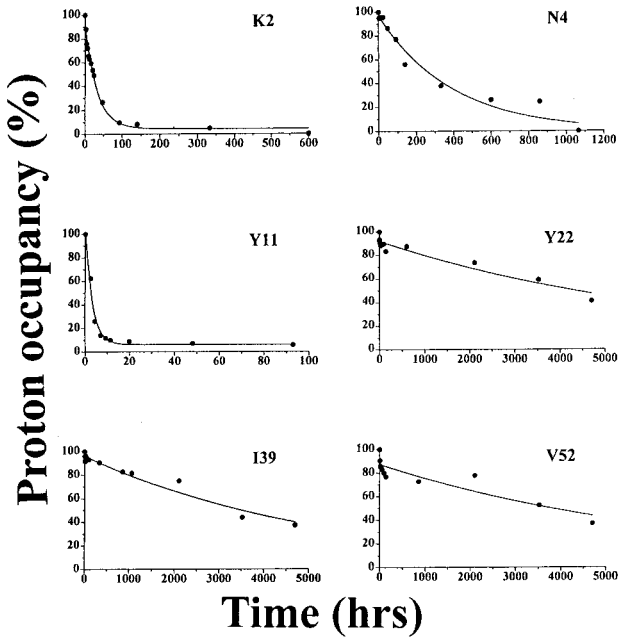

FIGURE 4: Changes in percentage of proton occupancy of some amide protons (at pD 3.6) involved in the secondary structure region(s).

The protection factors values of the various residues in CTX III, whose H/D exchange could be monitored, are shown in Table 1. For the sake of convenience, we arbitrarily classify the amide protons on the basis of protection factors as strongly ($P > 500$) and weakly ($P < 100$) protected from exchange. It could be observed that majority of the residues in the unstructured region of the molecule generally show weak ($P < 100$) protection against exchange. However, the residues in the C-terminal tail portion of the molecule extending from residues 57 to 59, show abnormally high ($P > 500$) protection. The protection factors of Asp57, Arg58, and Cys59 are comparable to many residues involved in the secondary structure formation. Similarly, Val27,

Table 1: Protection Factors and Time Constants of Refolding Residues in CTX III

residue	protection factor[a]	time constant (ms)	structural context	residue	protection factor[a]	time constant (ms)	structural context
Lys2	306	21.0 ± 02.2	strand I	Val32	61	163.9 ± 17.5	loop II
Cys3	2834	ND[b]	strand I	Val34	266	50.5 ± 04.3	loop II
Asn4	4436	ND	strand I	Lys35	7215	36.4 ± 10.0	strand IV
Lys5	421	33.0 ± 10.5	strand I	Arg36	56	32.1 ± 06.2	strand IV
Leu6	4	120.5 ± 08.7	loop I	Cys38	ND	35.6 ± 08.0	strand IV
Val7	50	52.4 ± 10.5	loop I	Ile39	40364	12.4 ± 00.9	strand IV
Leu9	3	ND	loop I	Val141	ND	161.3 ± 15.6	loop III
Phe10	5	36.9 ± 10.2	strand II	Cys42	96	ND	loop III
Tyr11	15	35.2 ± 11.7	strand II	Lys44	ND	49.5 ± 15.6	loop III
Lys12	17	33.7 ± 07.9	strand II	Ser46	5	ND	loop III
Lys18	68	80.8 ± 12.4	globular head	Leu48	1	129.9 ± 69.1	looop III
Asn19	3	ND	globular head	Val49	33	5.5 ± 01.2	loop III
Cys21	6996	27.6 ± 02.8	strand III	Tyr51	1055	12.7 ± 03.9	strand V
Tyr22	80289	30.8 ± 05.1	strand III	Val52	117082	11.8 ± 01.6	strand V
Lys23	11410	13.5 ± 02.0	strand III	Cys53	28	13.6 ± 02.7	strand V
Met24	13234	BD	strand III	Cys54	44646	ND	strand
Phe25	563	ND	strand III	Asn55	86	21.3 ± 05.0	strand V
Met26	981	ND	strand III	Asp57	684	9.8 ± 00.5	C-terminal
Val27	1380	ND	loop II	Arg58	4904	12.9 ± 03.0	C-terminal
Ala28	7	22.5 ± 03.2	loop II	Cys59	3816	172.4 ± 29.7	C-terminal
Thr29	ND	116.3 ± 09.5	loop II	Asn60	44	51.8 ± 09.4	C-terminal
Lys31	4	55.9 ± 13.1	loop II				

[a] The protection factor values have been rounded off to the closest whole number. [b] ND denotes that the data could not be detected.

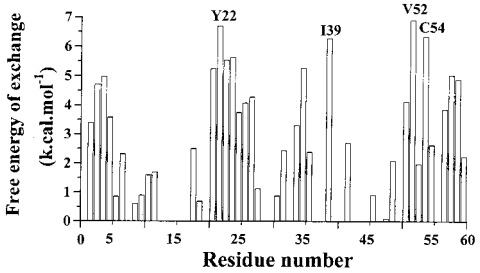

FIGURE 5: Plot depicting the free energy of exchange (ΔG_{ex}) of the various amide protons in CTX III. The four residues indicated in the figure possess ΔG_{ex} values higher than the average free energy of unfolding ($\Delta G_u = 6.0$ kcal·mol^{-1}).

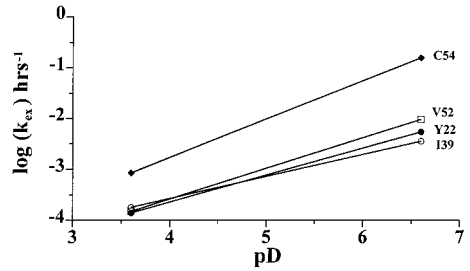

FIGURE 6: Representation of the differences in the amide proton exchange rate at pD 3.6 and 6.6. It could be discerned from the figure that exchange rates of the four residues (Tyr 22, Ile 39, Val 52, and Cys 54) show a strong pH dependence, implying that hydrogen−deuterium exchange for these four residues occurs by an EX2 mechanism.

located at the tip of loop 2, exhibits higher ($P > 500$) protection against exchange (Table 1). The residues located in the secondary structure region, in general, show high protection factor values. However, in comparison with the amide protons of residues belonging to the triple-stranded β-sheet segment, the residues involved in β-strand II of the double-stranded β-sheet segment show exceptionally low protection ($P < 100$). The residues lodged in β-strands III and V possess abnormally high protection factor values (Table 1). The protection factors for Tyr22, Lys23, Met24, Val52, and Cys54 are more than 10 000. Interestingly Val52 shows a protection factor value of 117 082.

For the majority of amide protons, ΔG_{ex} is smaller than ΔG_u (as determined by circular dichroism), indicating that these protons exchange from the native state ensembles under the conditions used (Figure 5). The free energy of exchange for Tyr22, Ile39, Val52, and Cys54 is greater by 0.1−0.9 kcal·mol^{-1} than the global free energy determined from equilibrium unfolding experiments with guanidine hydrochloride. Any meaningful estimation of the ΔG_{ex} must satisfy the conditions that the rate of conformational closing should be greater than the intrinsic exchange rate ($k_{cl} \gg k_{int}$). This is the EX2 limit. However, the observed rate of exchange (k_{ex}) would be the rate of the opening reaction, k_{op}, at the EX1 limit. This is due to the rate of conformational closing being less than the intrinsic exchange rate ($k_{cl} \ll k_{int}$). Under these circumstances (in the EX1 limit), it is impossible to procure information on the equilibrium constant for the opening reaction and hence the free energy of exchange. Thus, if the exchange occurs at the EX1 limit, the apparent free energy of exchange (ΔG_{ex}) can be higher than ΔG_u (*36*). To determine if the unexpected hydrogen exchange results of four residues (Tyr22, Ile39, Val52, and Cys54) is caused by an EX1 rather than an EX2 mechanism, we performed experiments to distinguish between the EX1 and EX2 limits. EX1 and EX2 are based on the principle that under EX1 conditions there is no pH dependence of the observed exchange rate, whereas if the exchange occurs in the EX2 limit, the rate of exchange (k_{ex}) is expected to be proportional to the concentration of H_3O^+ (or OH^-) in the acid (or the base) catalyzed reaction. A plot of k_{obs} for individual residues at different pH values differentiate the EX1 and EX2 limits (*35*). To examine the exchange through EX1 and EX2 limits in CTX III, the rate of amide exchange at pD 3.6 and 6.6 was measured under identical temperature conditions (25 °C). A plot of the logarithm of the rate of exchange versus the pD (Figure 6) depicts that rate of exchange for the four residues (Tyr22, Ile39, Val52, Cys54) at pD 6.6, in general,

is markedly higher (severalfold) than at pD 3.6. The exchange rate of four residues increases at least 20-fold upon raising the pD by 3 units.

The average ΔG_{ex} of the antiparallel double- and triple-stranded β-sheet segments in the protein are estimated to be 2.97 and 4.77 kcal·mol^{-1}, respectively. The average free energy of exchange (ΔG_{ex}) of the residues at the tips of the three loops in the proteins are estimated to be 1.26 (loop 1), 2.40 (loop 2), and 1.44 (loop 3) kcal·mol^{-1}. Although the C-terminal tail region (residues 56−60) is unstructured in the native state of CTX III, the residues 57−59 exhibit an unusually large average free energy (4.59 kcal·mol^{-1}) of exchange.

DISCUSSION

Relationship between H/D Exchange and Structure. Hydrogen−deuterium (H/D) exchange monitored by high-resolution NMR techniques provides useful insights on the internal dynamics of the native state (*35*). Amide protons with fast rates of exchange are substituted by solvent deuterons through local unfolding process. At the opposite extreme, exchange of the most protected amide protons in a globular protein would require a global unfolding of the protein with energy equal to the equilibrium denaturation free energy (*36*). In principle, the greater the protection of the amide proton from H/D exchange, the more stable is the local/global structure (*37*).

Protection factor(s) estimated from hydrogen−deuterium exchange experiments is a useful measure to evaluate the conformational stabilities of the backbone of protein molecules (*38*). The average protection factors of the five β-strands constituting the double- and triple-stranded β-sheet domains decrease in the order of β-strand V > β-strand III > β-strand IV > β-strand I > β-strand II. Conspicuously, residues in β-strand II show exceptionally weak protection against H/D exchange. Solution structures of CTX III depict a small twist in the backbone of the protein spanning residues in β-strand II (*27*, *28*). This twist probably increases the solvent exposure of the amide protons of residues (Phe10−Cys14) in β-strand II and accounts for their weak protection against H/D exchange. In contrast, residues (Lys2−Lys5) in β-strand I show more resistance against exchange. The amide protons of Cys3 and Asn4 show higher protection (P > 2500) factors because of their involvement in hydrogen bonding with the backbone carbonyl groups of Thr13 and Lys12, respectively. In addition, the occurrence of a high density of hydrogen bonds among the residues at the N- and C-terminal ends of the CTX III molecule also seems to aid in the stability of these hydrogen bonds (Cys3NH−Thr13CO and Asn4NH−Lys12CO) from solvent exchange.

It is interesting to note that some of the residues in the triple-stranded β-sheet domain such as Tyr22, Lys23, Met24, Ile39, Val52, and Cys54 show extraordinarily high protection (P > 10 000) against H/D exchange (Table 1). Solution structures of CTX III depict that β-strand III, which comprises Tyr22, Lys23, and Met24, is encircled by hydrophobic residues, namely, Leu6, Val7, Phe25, Val32, and Val34. This nonpolar core appears to effectively retard the permeation of the solvent (D_2O) molecules, rendering the amide protons of Tyr22, Lys23, and Met24 resistant to solvent exchange. In addition, the amide proton of Tyr22 is masked by the nonpolar side chains of Ile39 and Val41. This structural feature probably accounts for its (Tyr22) relatively higher protection (P > 80 000) than the other residues in β-strand III (*25*, *27*). Ile39 and Cys54 are two other residues in the triple-stranded β-sheet domain that exhibit strong protection (P > 40 000) against H/D exchange. Solution structures of CTX III show that the amide protons of these two residues are involved in backbone hydrogen bonding with Leu20CO and Cys21CO, respectively. In addition, these two residues occupy the head portion of the molecule, which is known to be very rigid with excessive cross-linking of the disulfide bonds (*3*−*21*, *14*−*38*, *42*−*53*, and *54*−*59*). This aspect ensures tight packing of the side chains of the various residues located in the head region of the molecule leading to the insulation of the hydrogen-bonded amide protons of Ile39 and Cys54 from solvent exposure.

Valine 52 exhibits the highest protection factor (P > 117 000) among the residues in CTX III. Val 52 is located in β-strand V and its amide proton is involved in a backbone interaction with Met24CO (*27*). Interestingly, the side chain of Val52 is sandwiched between two phenolic groups of Tyr22 and Tyr51 (*25*). This aspect is exemplified by strong ring current effects on the methyl protons of Val52. In addition, the presence of the disulfide bonds between Cys42 and Cys53 and between Cys54 and Cys59 confers rigidity to this portion (in the vicinity of Val52) of the CTX III molecule (*25*). These structural features almost impregnate the amide proton of Val52 and are predictably responsible for its slow exchange with the solvent (D_2O).

Some residues that are not located in the structured region(s) of the CTX III molecule show reasonably high (P > 500) protection factors. The amide proton of Val27, which is located in the structureless distal end of loop II, exhibits a high protection (P = 1380), probably due to hydrogen bonding with the carbonyl group of Leu48. This hydrogen bonding is crucial for bridging loops II and III of the toxin molecule (*38*, *39*). The close proximity of loops II and III is believed to be important for the lytic activity of snake venom cardiotoxins. An interesting feature observed in the H/D exchange of CTX III is the strong protection of the protons of residues (Asp57−Cys59) in the unordered C-terminal tail region of the molecule (*25*). The amide protons of residues in this region show protection factor values greater than 500. Solution structures of CTX III (*27*, *28*) reveal that the residues in the C-terminal loop are clustered due to the occurrence of a disulfide bond (Cys54−Cys59) and hydrogen bonds between Arg58NH and Cys59NH with the carbonyl groups of Lys2 and Cys3, respectively. Additionally, the side-chain amide group of Asn60 has long-range interactions with the backbone carbonyl groups of Cys21 and Tyr22, which reside in the triple-stranded β-sheet domain. Thus, the network of interactions among the residues located at the N-and C-termini compounded by the presence of a disulfide bond between Cys54 and Cys59 render the amide protons of these residues in the C-terminal significantly resistant to H/D exchange.

The amide proton exchange kinetics of CTX III provides useful information on the conformational stabilities of various regions in the toxin molecule. Comparison of the average protection factor and free energy of exchange of residues in double- ($P \sim 1148$, ΔG_{ex} = 2.97 kcal·mol^{-1}) and triple- ($P \sim 23\,143$, ΔG_{ex} = 4.77 kcal·mol^{-1}) stranded β-sheet

domain, unambiguously demonstrates that the triple-stranded β-sheet domain constitutes the central core region of the toxin molecule and contributes significantly to its global stability.

Hydrogen/Deuterium Exchange Mechanism. An examination of the standard free energy of the exchange (ΔG_{ex}) of the various residues in CTX III (Figure 5) shows that majority of the residues in the protein possess ΔG_{ex} values lower than the free energy change of unfolding (ΔG_u) obtained from the equilibrium unfolding experiments with circular dichroism spectroscopy. This aspect demonstrates that most of the residues in CTX III exchange by global unfolding. There are four residues in CTX III that show ΔG_{ex} values greater than the ΔG_u value (6.0 kcal·mol^{-1}). These residues include Tyr22 (6.69 kcal·mol^{-1}), Ile39 (6.28 kcal·mol^{-1}), Val52 (6.91 kcal·mol^{-1}) and Cys54 (6.34 kcal·mol^{-1}). The higher estimate of the standard free energy of exchange could sometimes be due to deviation from EX2 exchange kinetics. Deviation from EX2 kinetics has been observed for a few residues in barnase (*36*), hen egg white lysozyme (*40*), and turkey ovomucoid third domain (*41*). As vividly described by Niera et al. (*42*), a reliable method for detecting deviations from EX2 kinetics is an analysis of the relative effect of pD on the exchange rates of all amide protons. In principle, a plot of the logarithm of the exchange rates versus the pD can distinguish between EX2 and EX1, since k_{ex} is proportional to the hydroxide ion concentration. A plot of log k_{ex} versus the pD (Figure 6) for the four residues, namely, Tyr22, Ile39, Val52, Cys54, shows that the exchange rates at pD 6.6 are severalfold greater than the corresponding values at pD 3.6. This aspect indicates the higher ΔG_{ex} values over that of ΔG_u (for these four residues) is not due to deviation from the EX2 exchange kinetics.

In principle, under native conditions all possible states are accessible but the relative population given by the Boltzmann distribution (*22*), depends on the free energy of each state. Folding studies of CTX III have shown that only two states are significantly populated under all conditions: the native state ensemble and the unfolded state ensemble. As the mean free energy of protection for the globally exchanging residues of CTX III is almost similar to the free energy of unfolding (as determined from the ellipticity changes in the far-ultraviolet CD spectrum), the exchange of the four residues (wherein $\Delta G_{ex} > \Delta G_u$) possibly occurs from the fully unfolded state.

Is There a Relationship between Hydrogen Exchange and Folding Core? We have recently investigated the events in the refolding pathway of CTX III by a variety of techniques including quenched-flow hydrogen−deuterium exchange (*32*). The refolding of the protein was found to be completed within 200 ms. The secondary structural elements in the protein were found to be formed within the first 35 ms of refolding. The refolding kinetics of CTX III monitored by changes in ANS fluorescence has been demonstrated to proceed through occurrence of a hydrophobic collapse in the very early stages of refolding (burst phase).

Based on simultaneity between thermodynamic and kinetic aspects of protein folding observed in some proteins, Woodward and co-workers (*43*−*45*) proposed an interesting correlation between the exchange rates of amide protons and the sequence of events in a kinetic refolding pathway. They postulate (*45*) that the folding pathway approximates the reverse order of the native-state hydrogen exchange rates, i.e., the last hydrogen to exchange might identify the first part of the protein to fold—"last out, first in". Experimental data obtained on bovine pancreatic tyrosine inhibitor (*46*), cytochrome *c* (*47*), and lysozyme (*48*) showed a good relationship between native-state hydrogen exchange rates and the kinetic events in protein folding pathways. Recently, Lacroix et al. (*49*), comparing the equilibrium amide proton exchange kinetics with the events in the folding pathway of the chemotactic protein (CheY) from *Escherichia coli*, using a quenched-flow technique, revealed that the highest protection from hydrogen exchange is a part of the folding nucleus. Chamberlain and Marqusee (*50*) identified two high-energy, partially unfolded intermediates in RNase H through native-state H/D exchange methods. Impressive evidence exists on the occurrence of these high-energy kinetic intermediates in the kinetic refolding pathway of this protein (RNase H, *51*). More recent work on barnase (*52*) and chymotrypsin inhibitor (CI2, *53*) showed that some regions that are formed early in the folding reaction do not belong to the group of slowest-exchanging protons. Tertiary structure interactions, known to be formed late during the folding pathway, involved some of the slowest exchange protons in these proteins (*54*). In addition, H/D exchange kinetics in CI2 also revealed that the α-helix at the N-terminus is not among the set of slowest-exchanging protons (*53*).

Comparison of the results of the native-state H/D exchange kinetics obtained in the present study and the quenched-flow deuterium exchange data on the refolding kinetics of CTX III (*32*) provides us a good opportunity to examine if there exists a relationship between slowly exchanging regions and the folding nucleus of the protein. In general, in CTX III, there is a good correlation between the residues that exhibit the slowest exchange from the native state and those that are rapidly protected during the initiation of folding. Refolding kinetics of CTX III monitored by quenched-flow H/D exchange revealed that the double- and triple-stranded β-sheet segments in the protein are formed with average time constants of 35 and 19.7 ms, respectively (*32*). Correspondingly, the average protection factors of the double- and triple-stranded β-sheet domains have been estimated to be 1148 and 23 143, respectively. Thus, the data appears to agree well with the "last out, first in" hypothesis. In addition, among the three strands comprising the triple-stranded β-sheet domain, β-strand V has been found to fold fastest with an average folding time constant of 17.2 ± 2.7 ms. Interestingly, the protection factor for β-strand V is the largest (Table 1) in the triple-stranded β-sheet domain. This aspect is in conformity with the "last out, first in" hypothesis proposed by Woodward and co-workers (*43*−*45*).

Table 1 shows that most of the residues with low protection factors fold slowly (with higher time constant values) during the refolding process of the protein. The amide proton of Val49 is involved in a backbone hydrogen bonding with Ser46CO forming a type 1β turn. Interestingly, Val49 shows the lowest time constant value (5.5 ms, Table 1), implying that the formation of the type 1β turn between Val49NH and Ser46CO is among the earliest events detected in the refolding pathway of CTX III. Paradoxically, the amide proton of Val49 is found to exhibit relatively weak protection ($P \approx 33$) against hydrogen−deuterium exchange.

Barring a few exceptions such as Val49, the hydrogen−deuterium exchange data obtained in this study seem to

suggest (at least in CTX III) that the slowly exchanging residues constitute the protein folding core of the protein. It should be emphasized that the results obtained in this study cannot be extrapolated to judge the general validity of the "last out, first in" hypothesis. There is no automatic relationship between the hydrogen exchange at equilibrium and the protein-folding pathway. To determine the sequence of events in the refolding pathway, kinetic measurements must be made. We have recently cloned and expressed CTX III (*55*) in high yields, and experiments are underway to further understand the role of various residues in the stability and folding of the protein.

ACKNOWLEDGMENT

We express our sincere thanks to the anonymous reviewers for their useful comments. We also acknowledge the Regional Instrumental Center, Hsinchu, for allowing us to use the 600 MHz NMR spectrometer.

REFERENCES

1. Dalby, P. A., Clarke, J., Christopher, M. J., and Fersht, A. R. (1998) *J. Mol. Biol. 276*, 647−656.
2. Bai, Y., Sosnick, T. R., Mayne, L., and Englander, S. W. (1995) *Proteins: Struct., Funct., Genet. 17*, 75−86.
3. Englander, S. W., and Kallenbach, N. R. (1984) *Q. Rev. Biophys. 16*, 521−655.
4. Woodward, C., Simon, I., and Tuchsen, E. (1982) *Mol. Cell. Biochem. 48*, 135−160.
5. Englander, S. W., Downes, N. W., and Teitebaum, H. (1972) *Annu. Rev. Biochem. 41*, 903−924.
6. Miller, D. W., and Dill, K. A. (1995) *Protein Sci. 4*, 1860−1873.
7. Hillser, V. J., and Freire, E. (1996) *J. Mol. Biol. 262*, 756−772.
8. Bai, Y., and Englander, S. W. (1996) *Proteins: Struct., Funct., Genet. 24*, 145−151.
9. Kargelund, B. B., Knudsen, J., and Poulsen, F. M. (1995) *J. Mol. Biol. 250*, 695−706.
10. Clarke, J., and Itzhaki, L. S. (1998) *Curr. Opin. Struct. Biol. 8*, 695−706.
11. Thomsen, N. K., and Poulsen, F. M. (1993) *J. Mol. Biol. 234*, 24−241.
12. Marmoino, J., Auld, D. S., Betz, S. F., Doyle, D. F., Young, G. B., and Pielak, G. J. (1993) *Protein Sci. 2*, 1966−1974.
13. Englander, S. W., Sosnick, T. R., Englander, J. J., and Mayne, L. (1996) *Curr. Opin. Struct. Biol. 6*, 18−25.
14. Pedersen, S., Clarke, J., Hounslow, A. M., and Fersht, A. R. (1995) *Biochemistry 24*, 7396−7407.
15. Hvidt, A. A., and Nielsen, S. O. (1996) *Adv. Protein Chem. 21*, 287−386.
16. Bahar, I., Wallquest, A., Corell, D. G., and Jernigen, R. L. (1998) *Biochemistry 37*, 1067−1075.
17. Woodward, C., and Hilton, B. (1980) *Biophys. J. 32*, 560−572.
18. Loh, S. N., Rohl, C. A., Kiefhaber, T., and Baldwin, R. L. (1996) *Proc. Natl. Acad. Sci. U.S.A. 93*, 1982−1987.
19. Amington, C. B., and Robertson, A. D. (1997) *Biochemstry 36*, 8686−8691.
20. Qian, H., Mayo, S. L., and Motron, A. (1994) *Biochemistry 33*, 8161−8171.
21. Mullins, L., Pau, C. N., and Raushel, F. M. (1997) *Protein Sci. 6*, 1387−1395.
22. Bai, Y., Milne, J. S., Mayne, L., and Englander, S. W. (1995) *Science 269*, 192−197.
23. Chamberlain, A. K., and Marqusee, S. (1997) *Structure 5*, 859−863.
24. Johnson, C. M., and Fersht, A. R. (1995) *Biochemistry 34*, 6795−6804.
25. Kumar, T. K. S., Jayaraman, G., Lee, C. S., Arunkumar, A. I., Sivaraman, T., Samuel, D., and Yu, C. (1997) *J. Biomol. Struct. Dyn. 15*, 431−463.
26. Kumar, T. K. S., Lee, C. S., and Yu, C. (1995) in *Natural toxins II* (Singh, B. R., and Yu, C., Eds.) pp 114−129, Plenum Press, New York.
27. Bhaskaran, R., Huang, C. C., Chang, D. K., and Yu, C. (1994) *J. Mol. Biol. 235*, 129−135.
28. Sivaraman, T., Kumar, T. K. S., Huang, C. C., and Yu, C. (1998) *Biochem. Mol. Biol. Int. 44*, 29−39.
29. Chang, J. Y., Kumar, T. K. S., and Yu, C. (1998) *Biochemistry 37*, 6745−6751.
30. Kumar, T. K. S., Pandian, S. K., Srisailam, S., and Yu, C. (1998) *J. Toxicol. Toxin Rev. 17*, 183−212.
31. Sivaraman, T., Kumar, T. K. S., Jayaraman, G., and Yu, C. (1997) *Biochem. J. 321*, 457−464.
32. Sivaraman, T. Kumar, T. K. S., Cheng, D. K., Lin, W. Y., and Yu, C. (1998) *J. Biol. Chem. 273*, 10081−10093.
33. Yang, C. C., King, K., and Sun, T. P. (1981) *Toxicon 19*, 645−659.
34. Pace, C. N. (1986) *Methods Enzymol. 131*, 266−280.
35. Bai, Y., Milne, J. S., Mayne, L., and Englander, S. W. (1993) *Proteins: Struct., Funct., Genet. 17*, 75−86.
36. Perret, S., Clarke, J., Hounslow, A. M., and Fersht, A. R. (1995) *Biochemistry 34*, 9288−9299.
37. Wagner, G. (1980) *Biochem. Biophys. Res. Commun. 97*, 614−620.
38. Menez, A., Gafinear, E., Roumestand, C., Harvey, A. L, Monwad, L., Gilquin, B., and Toma, F. (1990) *Biochemie 72*, 575−588.
39. Gilquin, B., Roumestand, C., Justin, Z. S., Menez, A., and Toma, F. (1993) *Biopolymers 33*, 1659−1675.
40. Radford, S. E., Buck, M., Topping, K. D., Dobson, C. M., and Evans, P. A. (1993) *Proteins: Struct., Funct., Genet. 14*, 237−248.
41. Swint, L., and Robertson, A. D. (1993) *Protein Sci. 2*, 2037−2049.
42. Niera, J. L., Itzaki, L. S, Otzen, D. E., Davis, B., and Fersht, A. R. (1997) *J. Mol. Biol. 270*, 99−110.
43. Kim, K. S., and Woodward, C. (1993) *Biochemistry 32*, 9609−9613.
44. Woodward, C. (1993) *Trends Biochem. Sci. 18*, 359−360.
45. Kim, K. S., Fuchs, J. A., and Woodward, C. K. (1993) *Biochemistry 32*, 9600−9608.
46. Roder, H., and Wuthrich, K. (1988) *Proteins: Struct., Funct., Genet. 1*, 34−42.
47. Roder, H., Elove, G., and Englander, S. W. (1988) *Nature 335*, 700−704.
48. Radford, S. E., Dobson, C. M., and Evans, P. (1992) *Nature 358*, 302−307.
49. Lacroix, E., Bruix, M., Lopez-Hernandez, E., Serrano, L., and Rico, M. (1997) *J. Mol. Biol. 271*, 472−487.
50. Chamberlain, A. K., and Marqusee, S. (1998) *Biochemistry 37*, 1736−1742.
51. Raschke, T. M., and Marqusee, S. (1997) *Nat. Struct. Biol. 4*, 298−304.
52. Clerke, J., and Fersht, A. R. (1996) *Folding Des. 1*, 243−254.
53. Itzaki, L. S., Niera, J. L., and Fersht, A. R. (1997) *J. Mol. Biol. 270*, 89−98.
54. Clarke, J., Itzhaki, L. S., and Fersht, A. R. (1997) *Trends Biochem. Sci. 22*, 284−287.
55. Kumar, T. K. S., Yang, P. W., Lin, S. H., Wu, C. Y., Lei, B., Lo, S. J., Tu, S. C., and Yu, C. (1996) *Biochem. Biophys. Res. Commun. 219*, 450−456.

BI9901230